Ellipticals at $z = 0$ from Self-Consistent Hydrodynamical Simulations: Comparison with SDSS Structural and Kinematical Data

A. Sáiz[1], R. Domínguez-Tenreiro [1] and A. Serna [2]

ABSTRACT

We present results of an analysis of the structural and kinematical properties of a sample of elliptical-like objects (ELOs) identified in four hydrodynamical, self-consistent simulations run with the DEVA code (Serna et al. 2003). Star formation has been implemented in the code through a simple phenomenological parameterization, that takes into account stellar physics processes only implicitly through the values of a threshold gas density, $\rho_{\rm g,thres}$, and an efficiency parameter, c_*. The four simulations operate in the context of a ΛCDM cosmological model consistent with observations, resolve ELO mass assembly at scales up to $\simeq 2$ kpc, and differ in the values of their star formation parameters. Stellar masses, projected half-mass radii and central l.o.s. velocity dispersions, $\sigma_{\rm los,0}$, have been measured on the ELO sample and their values compared with data from the Sloan digital sky survey. For the first time in self-consistent simulations, a good degree of agreement has been shown, including the Faber-Jackson and the $D_n - \sigma_{\rm los,0}$ relations, among others, but only when particular values of the $\rho_{\rm g,thres}$ and c_* parameters are used. This demostrates the effect that the star formation parameterization has on the ELO mass distribution. Additionally, our results suggest that it is not strictly necessary, at the scales resolved in this work, to appeal to energy sources other than gravitational (as for example supernovae feedback effects) to account for the structure and kinematics of large ellipticals.

Subject headings: cosmology: theory - galaxies: ellipticals - galaxies: formation - galaxies: fundamental parameters - hydrodynamics

[1]Dpt. Física Teórica C-XI, Universidad Autónoma de Madrid, E-28049 Cantoblanco, Madrid, Spain; e-mail: alejandro.saiz@uam.es, rosa.dominguez@uam.es

[2]Dpt. Física y A.C., Universidad Miguel Hernández, E-03206 Elche, Alicante, Spain; e-mail: arturo.serna@umh.es

1. INTRODUCTION

One of the most challenging open problems in modern cosmology is the origin of the local galaxies of different Hubble types we observe to-day. Among them, ellipticals are the easiest to study. They form the most homogeneous family and show the most precise regularities in the form of correlations among some pairs of their observable parameters. The Sloan digital sky survey (SDSS, see York et al. 2000) sample of early-type galaxies, containing to date 9000 galaxies from different environments, provides a new standard of reference for nearby elliptical galaxies. Its analysis confirmed correlations previously established, such as those involving structural and kinematical parameters (the $L - \sigma_{\rm los,0}$ or Faber-Jackson relation, 1976; the surface-brightness - effective radius relation, Kormendy 1977; the $D_n - \sigma_{\rm los,0}$ relation, Dressler et al. 1987; among others, see Bernardi et al. 2003a, 2003b, 2003c, 2003d, and references quoted therein). These correlations, as well as the [α/Fe] ratio trend with $\sigma_{\rm los,0}$ (Jorgensen 1999), demand short formation time-scales and old formation ages for the bulk of the stellar populations of ellipticals. These requirements are naturally met by one of the scenarios proposed so-far to explain galaxy formation and evolution: the so-called *monolithic collapse* scenario (ellipticals would form at high z in a single burst of star formation, and would passively evolve since then; Patridge & Peebles 1967; Larson 1974). The competing *merging scenario* (galaxy mass assembly takes place gradually through repeated mergers of smaller subunits; Toomre 1977; Kauffmann 1996) meets some difficulties at explaining the correlations above as well as other observations on ellipticals, see Peebles 2002 and Matteucci 2003 for details and discussions. But the monolithic collapse scenario does not recover all the currently available observations on ellipticals either. Such are, for example, the range in ages their stellar populations span in some cases or their kinematical and dynamical peculiarities (Trager et al. 2000; Menanteau, Abraham & Ellis 2001), indicating that an important fraction of present-day ellipticals have recently experienced merger events.

In order to reconcile all this observational background within a formation scenario, it is preferable to study galaxy assembly from simple physical principles and in connection with the global cosmological model. Self-consistent gravo-hydrodynamical simulations are a very convenient tool to work out this problem (Navarro & White 1994, Tissera, Lambas & Abadi 1997, Thacker & Couchman 2000). The method works as follows: initial conditions are set at high z as a Montecarlo realization of the field of primordial fluctuations to a given cosmological model in a periodic, homogeneously sampled box; then the evolution of these fluctuations is numerically followed up to $z = 0$ by means of a computing code that solves the N-body plus hydrodynamical evolution equations. In this way, the uncertainties resulting from prescriptions on dynamics and gas cooling and heating, present in other methods such as semi-analytical ones (Kauffmann et al. 1999, Mathis et al. 2002) can be removed, only star formation needs further modelling. Individual galaxy-like objects (GLOs) natu-

rally appear as an output of the simulations, no prescriptions are needed as far as their mass assembly processes are concerned. Moreover, self-consistent simulations directly provide detailed information on each individual GLO at each z, namely its six dimensional phase space structure, as well as the temperature and age distributions of its gaseous and stellar components, respectively. From this information, the parameters characterizing each GLO can be estimated and compared with observations (see, for example, Sáiz et al. 2001, concerning disk galaxies). The first step in the program of studying the origin of galaxies through self-consistent simulations, is to make sure that they form GLO samples of different Hubble types that have counterparts in the real local Universe. In particular, the possible simple correlations involving structural and kinematical parameters must be recovered. A detailed analysis of this kind was not yet available for ellipticals (see previous work in Kobayashi 2002; Sommer-Larsen, Gotz, & Portinari 2002; Meza et al. 2003).

We present in this paper the results of an analysis of the structure and kinematics of a sample of elliptical-like objects (ELOs) identified in four self-consistent hydrodynamical simulations run in the framework of a flat ΛCDM model consistent with observations. We have used DEVA, an AP3M-SPH code particularly designed to study galaxy assembly in a cosmological context. In DEVA, special attention has been paid that the implementation of conservation laws (energy, entropy and angular momentum) is as accurate as possible (see Serna, Domínguez-Tenreiro, & Sáiz, 2003 for details, in particular for a discussion on the observational implications of violating some conservation laws). Star formation (SF) processes have been implemented in the code through a simple parameterization, similar to that first used by Katz (1992), that includes a threshold gas density, $\rho_{\rm g,thres}$ and an efficiency parameter, c_*, determining the SF timescales according with a Kennicutt-Schmidt law[3] (Kennicutt 1998).

Galaxy-like objects of different morphologies have been identified in the simulations (Sáiz, Domínguez-Tenreiro & Serna 2002; Sáiz 2003). The aim of this paper is to show that some of those identified as ELOs, have, at a structural and kinematical level, counterparts in the local Universe, including parameter correlations. Data have been taken from the SDSS as analyzed by Bernardi et al. (2003a, 2003b), Kauffmann et al. (2003a, 2003b) and Shen et al., 2003. A brief account on ELO assembly is as follows: it mainly occurs through a multiclump collapse at rather high z involving many clumps; collapse takes the clumps closer and closer along filaments causing them to merge at very low relative angular

[3]See Elmegreen (2003) for a discussion on the possibility that this law can be explained as a result of SF processes at the scale of molecular cloud cores, through an interstellar medium (ISM) gas structure whose density, prior to SF, can be described by a log-normal probability distribution, as Wada & Norman (2001) found in their simulations

momentum and, consequently, at short timescales. This results into fast SF bursts at high z that transform most of the available gas into stars. The frequency of head-on mergers decreases with z. ELO stellar populations are mostly old, and a trend exists with $\sigma_{\rm los,0}$, as suggested by some observations (Thomas, Maraston & Bender, 2002).

2. OBJECTS AT $z = 0$

We have analyzed ELOs identified in four different simulations, namely S14, S16, S17 and S26, run within the same global flat Λ cosmological model, with $h = 0.65$, $\Omega_{\rm m} = 0.35$, $\Omega_{\rm b} = 0.06$. The normalization parameter has been taken slightly high, $\sigma_8 = 1.18$, as compared with the average fluctuations of 2dFGRS or SDSS galaxies (Lahav et al. 2002, Tegmark et al. 2003) to mimic an active region of the Universe (Evrard, Silk & Szalay 1990). The gravitational resolution is $\epsilon_{\rm g}$= 2.3 kpc. Feedback effects from stellar processes have not been explicitly included in the simulations, but the values of the SF parameters we use mimic them in a sense [4]. S14, S16, and S26 share the same initial conditions (their assembly histories are identical at halo scales) and differ only in the SF parameters ($c_* = 0.1$, 0.03 and 0.01, and $\rho_{\rm g,thres} = 6 \times 10^{-25}, 1.8 \times 10^{-24}, 6 \times 10^{-24}$ gr cm^{-3} for S14, S16 and S26, respectively, that is, SF becomes increasingly more difficult from S14 to S26), to test the effects of SF parameterization to shape ELOs. S17 is identical to S16, except that their initial conditions differ, to test cosmic variance. A standard cooling function has been used. Each of the four simulations started at a redshift $z_{\rm in} = 20$. In any run, 64^3 dark matter and 64^3 baryon particles, with a mass of 1.29×10^8 and $2.67 \times 10^7 {\rm M}_\odot$, respectively, have been used to homogeneously sample the density field in a periodic box of 10 Mpc side. The mass function of galaxy-like objects formed in this box is consistent with that of a small group environment (Cuesta-Bolao & Serna, private communication), where the efficiency of galaxy formation per volume unit is higher than average in the universe, and, so, the fraction of cold baryons (i.e., cold gas and stars) in the box is also higher than average. ELOs have been identified as those objects having a prominent stellar spheroidal component with hardly disks at all (Sáiz 2003; Sáiz et al., in preparation). The 8 more massive objects identified at $z = 0$ in S14, S16 and S17, and the 4 more massive in S26, fulfill this condition. The most (least) massive object in the sample has, at $z = 0$, 59,300 (4,130) dark and 29,600 (2,610)

[4]Note that the role of stellar processes at kpc scales is not yet clear, as some authors argue that their energy release drives the structure of the ISM locally at sub-kpc scales, while gas compression processes other than stellar pressures, for example gravitational instabilities, structure the gas prior to SF at scales $\geq$ kpc (Elmegreen, 2003). Our ignorance of sub-kpc (that is, subresolution) scale processes, including SNe feedback effects, is circumvented by taking them implicitely into account through the SF parameterization

baryon particles within its virial radius. The spin parameters of the ELO sample have an average value of $\bar{\lambda} = 0.033$. Their stellar components have ellipsoidal shapes, and, in most cases, they are dynamically relaxed systems.

The 3D stellar mass density profiles are steeper than those of dark matter (DM) as a result of energy losses by gas particles as they cool and fall onto the center of the configuration. The size scales are closely correlated to the halo mass scale, $M_{\rm vir}$; they also depend on the SF parameters, because the easier it is for a gas particle in a given proto-ELO to be transformed into a stellar particle, the lower the amount of energy it will radiate before being transformed, and, so, the lower the total dissipation ensuing the ELO formation. Concerning ELO velocity distributions, their 3D structure is such that stars and dark matter do not exhibit a global rotation; the stellar velocity dispersion profiles are systematically lower than DM ones (as found by Loewenstein 2000 on theoretical grounds) and they slightly decrease outwards; the anisotropy parameter is always positive, that is, disordered energy lies preferentially on radial motions. Projected mass and velocity distributions can be characterized by global mass (i.e., luminosity), size and velocity dispersion parameters that have been extensively observed in real ellipticals and can be easily measured in simulated ELOs, making the comparison with observational data possible. Physically, the mass parameter at the ELO scale is $M_{\rm bo}^{\rm cb}$, the total amount of cold baryons that have reached the central $\sim$ few kpc volume of the halos, forming an ELO. A fraction of these cold baryons have turned into stars, depending on the strength of the dynamical activity in the volume surrounding the proto-ELO at high z, and, also, on the efficiency of the SF algorithm. $M_{\rm bo}^{\rm star}$ is the stellar mass. Hereafter we will only refer to $M_{\rm bo}^{\rm star}$ as mass scale, as it can be estimated from luminosity data through modelling (Kauffmann et al. 2003a, for example). Note that S14 objects have a slightly higher stellar content than S26 objects, with those from S16 and S17 at intermediate positions, as expected due to the values of their SF parameters. The projected effective *mass* radius, $R_{\rm e,bo}^{\rm star}$, is the radius enclosing a mass equal to $M_{\rm bo}^{\rm star}/2$ as seen in projection. Observationally, a useful characterization of the velocity dispersion of an elliptical galaxy is provided by its central line-of-sight velocity dispersion, $\sigma_{\rm los,0}$. It has been measured in the ELO sample and found to be tightly correlated with $M_{\rm vir}$.

Our next concern is related with the extent to which ELOs in the sample as described by $M_{\rm bo}^{\rm star}$ as mass parameter, $R_{\rm e,bo}^{\rm star}$ as projected size parameter, and $\sigma_{\rm los,0}$ as velocity dispersion parameter, have observational counterparts. On the observational side, Bernardi et al. (2003b) provide maximum-likelihood estimates of the parameters characterizing the joint probability distribution (a trivariate gaussian) for absolute luminosities, M, (the logarithms of) intrinsic sizes, R, and central velocity dispersions, V, namely, their mean values and the covariance matrix. Stellar masses of a sample of 10^5 SDSS galaxies of different morphological types have been estimated by Kauffmann et al. (2003a). Their results indicate

that the stellar-mass-to-light ratio, S, can be taken to be constant in the range of absolute luminosities $M < -21$, that is, for the more massive or, equivalently, early-type galaxies in their sample (see Kauffmann et al. 2003b). The values of the logarithm of this ratio are $S \simeq 0.53$ and $S \simeq 0.25$, with dispersions $\sigma_S < 0.15$ and 0.1, in the r and z SDSS bands, respectively. The independence of the value of S with M implies that the pairwise correlation coefficients, $\rho_{\rm SM}$, can be taken $\simeq 0$ to a good accuracy. Assuming, moreover, that the pairwise correlation coefficients $\rho_{\rm SR}$ and $\rho_{\rm SV}$, are also $\simeq 0$, the pairwise concentration ellipses (and regression lines) can be drawn for the same data variables as those we have measured on simulated ELOs (that is, stellar masses instead of absolute luminosity, R and V). This allows us to do a more meaningful comparison.

In Figure 1, the consistency between SDSS data and ELOs as seen in the $\sigma_{\rm los,0}$ versus $R^{\rm star}_{\rm e,bo}$ plot is addressed. Points are ELO measured values, with different symbols for different simulations. The ellipse is the 2σ concentration ellipse and the lines are its major and minor axes for the SDSS early-type galaxy sample in the z band (the other SDSS bands lead to almost identical data diagrams). We recall that the major axis corresponds to the orthogonal mean square regression line, o.m.s.r.l., for the two variables in the Figure, and that the 1σ (2σ) region from the o.m.s.r.l. can be drawn by tracing its parallel lines through the middle (end) points of the minor semiaxis; they have not been drawn in the Figure for the sake of clarity. We see that, except for 5 of the S14 ELOs, the whole ELO sample lies within the 2σ concentration ellipse. The effects of the different SF parameterizations are apparent in this plot. We see that while those ELOs formed in simulations where SF is easy (S14), tend to be too large for their $\sigma_{\rm los,0}$ and outside the 1σ (or even the 2σ) o.m.s.r.l. region, those formed in simulations where SF is difficult (S26), tend to be smaller for their velocity dispersion. ELOs formed in S16 and S17 have intermediate sizes and agree with SDSS data at 1σ level, showing a power-law correlation (the $D_n - \sigma_{\rm los,0}$ relation). This behaviour with the SF parameterization is consistent with the interpretation that the easier to form stars, the lower the amount of energy lost by the gas before being turned into stars.

In Figure 2 we plot the stellar half-mass radii, $R^{\rm star}_{\rm e,bo}$, versus the stellar masses, $M^{\rm star}_{\rm bo}$. Data are the median values (points) and 1 sigma dispersions (error bars) for the distribution of Sérsic (1968) half-light radius in the z-band as a function of stellar mass for SDSS early-type galaxies (Shen et al. 2003, their Figure 11; data in the r-band do not differ substantially). We have also plot the 2σ concentration ellipse drawn from Bernardi et al.'s sample as explained above. The vertical line stands for the lower bound of early-type galaxy stellar masses, as found by Kauffmann et al. 2003b. We first note that, when, say, $M^{\rm star}_{\rm bo} > 6 \times 10^{10} M_\odot$, the consistency of data analysis by Shen et al. 2003 and Bernardi et al. 2003 is remarkable. Comparing Shen et al. 2003 results and our simulations in this mass range, we see that the agreement is good at a 1σ level for S14 ELOs (even if they are larger

than median data values), as well as for the S17 and S16 ELO sample (smaller than median data values), except for three of them, that are within 2σ of Shen et al.'s data. In this range of stellar mass, $R_{\rm e,bo}^{\rm star}$ and $M_{\rm bo}^{\rm star}$ show a power law correlation with a low dispersion and an exponent and zero point consistent with data. For lower masses, S17 and S16 ELOs are too small for their stellar masses at 1σ, as are S26 ELOs in any range of stellar mass. The effects of the SF parameterization on this plot are similar to those on Figure 1 we have just discussed.

Finally, we analyze the consistency between simulations and data from the $\sigma_{\rm los,0}$ versus $M_{\rm bo}^{\rm star}$ plot (Figure 3). We draw points for results of ELO measurements and the 2σ concentration ellipse for SDSS data. We see that most of the ELO sample lies within this ellipse, even if ELOs, and particularly so the less massive ones, tend to have rather high stellar masses for their $\sigma_{\rm los,0}$ as compared with SDSS galaxies in the same $\sigma_{\rm los,0}$ range. Most ELOs with $M_{\rm bo}^{\rm star} > 10^{11} M_\odot$, are inside the 1σ o.m.s.r.l. region for SDSS data, and they show a power-law relation with slope and zero point consistent with data and with low dispersion (note that as $M^{\rm star}/L$ is constant, this is just the Faber-Jackson relation). The dispersion is even lower for S17 and S16 ELOs with, say, $M_{\rm bo}^{\rm star} > 6 \times 10^{10} M_\odot$ when taken alone. Note that, even if most S14 objects have higher values of $M_{\rm bo}^{\rm star}$ than their S26 counterparts, with S16 and S17 objects at an intermediate position, all the objects follow the same relation, and particularly so the most massive ones, so that the different SF parameterizations have no important effects on this plot as far as the correlation is concerned.

3. Discussion

The degree of consistency reported here between sizes, velocity dispersions and stellar masses of simulated ELOs and SDSS data is very good. The agreement is particularly outstanding when the simplicity of our working scheme is recalled: ELO assembly has been simulated in the context of a cosmological model roughly consistent with observations; Newton laws and hydrodynamical equations have been integrated in this context, with a standard cooling algorithm and a SF parameterization through a Kennicutt-Schmidt-like law, containing our ignorance about its details at sub-kpc scales. No further hypotheses to model the assembly processes have been made. Our results suggest that, at least for the more massive objects, say $\geq 6 \times 10^{10}$ $M_\odot$, it is not strictly necessary to appeal to energy sources, *at the scales resolved in this work*, that is, up to ~ 2 kpc, other than gravitational to account for their sizes, velocity dispersions, stellar masses and their correlations. This result is consistent with the idea that SNe explosions are not relevant at these scales, but only at smaller scales, to make shells and trigger star formation in molecular cloud cores. Their effect would be

accounted for in the SF parameters (Elmegreen 2003).

This work strongly suggests that the SF parameterization is a key ingredient to determine the compactness of elliptical galaxies. A good agreement has been found in the correlations addressed here with SDSS data, but in the case of those involving sizes, only when particular values of the SF parameters are used. Our results push the problem of elliptical galaxy formation from understanding their mass assembly at scales $>$ kpc in a cosmological context (Domínguez-Tenreiro et al. 2003, in preparation), to understanding how SF was regulated at high z as the gas falls within collapsing volumes, or other shock locations, so as to proceed just with the efficiency necessary to produce the sizes observed in to-day ellipticals.

It is a pleasure to thank J. Silk and J. Sommer-Larsen for useful information on the topics addressed in this paper. This work was partially supported by the MCyT (Spain) through grant AYA-0973 from the Programa Nacional de Astronomía y Astrofísica. We also thank the Centro de Computación Científica (UAM, Spain) for computing facilities.

REFERENCES

Bernardi, M., et al. 2003a, AJ, 125, 1817; 2003b, AJ, 125, 1849; 2003c, AJ, 125, 1866

Bernardi, M., et al. 2003d, AJ, 125, 1882

Dressler, A., Lynden-Bell, D., Burstein, D., Davies, R. L., Faber, S. M., Terlevich, R., & Wegner, G. 1987, ApJ, 313, 42

Elmegreen, B. 2003, Ap&SS, 284, 819

Evrard, A., Silk, J., & Szalay, A.S. 1990, ApJ, 365, 13

Faber, S. M., & Jackson, R. E. 1976, ApJ, 204, 668

Jorgensen, I. 1999, MNRAS, 306, 607

Katz, N. 1992, ApJ, 391, 502

Kauffmann, G. 1996, MNRAS, 281, 475

Kauffmann, G., Colberg, J.M., Diaferio, A., & White, S.D.M., 1999, MNRAS, 303, 188

Kauffmann, G., et al., 2003a, MNRAS, 341, 33

Kauffmann, G., et al., 2003b, MNRAS, 341, 54

Kennicutt, R. 1998, ApJ, 498, 541

Kobayashi, C. 2002, Ap&SS, 281, 301

Kormendy, J. 1977, ApJ, 218, 333

Lahav, O., et al. 2002, MNRAS, 333, 961L

Larson, R. B. 1975, MNRAS, 164, 585

Loewenstein, M. 2000, ApJ, 532, 17

Mathis, H., Lemson, G., Springel, V., Kauffmann, G., White, S.D.M., Eldar, A., & Dekel, A. 2002, MNRAS, 333, 739

Matteucci, F. 2003, Ap&SS, 284, 539

Menanteau, F., Abraham, R.G., & Ellis, R.S. 2001, MNRAS, 322, 1

Meza, A., Navarro, J., Steinmetz, M., & Eke, V.R., 2003, ApJ, 590, 619

Navarro, J.F., & White, S.D.M., 1994, MNRAS, 267, 401

Partridge, R.B., & Peebles, P.J.E. 1967, ApJ, 147, 868

Peebles, P.J.E. 2002, in A New Era in Cosmology, ASP Conf., eds. N. Metcalf and T. Shanks

Sáiz, A., Domínguez-Tenreiro, R., Tissera, P.B., & Courteau, S. 2001, MNRAS, 325, 119

Sáiz, A., Domínguez-Tenreiro, R., & Serna, A. 2002, Ap&SS 281, 309

Sáiz, A. 2003, PhD, Universidad Autónoma de Madrid

Serna, A., Domínguez-Tenreiro, R., & Sáiz, A. 2003, ApJ in press, astro-ph/0307312 preprint

Sérsic, J.L. 1968, Atlas de galaxias australes (Córdoba, Argentina: Observatorio Astronómico)

Shen, S., et al. 2003, MNRAS, 343, 978

Sommer-Larsen, J., Gotz, M., & Portinari, L. 2002, astro-ph/0204366 preprint

Tegmark, M., et al. 2003, astro-ph/0310723 preprint

Thacker, R.J., & Couchman, H.M.P. 2000, ApJ, 545, 728

Thomas, D., Maraston, C., & Bender, R. 2002, R.E. Schielicke (ed.), Reviews in Modern Astronomy, Vol. 15, Astronomische Gesellschaft, astro-ph/0202166 preprint

Tissera, P.B., Lambas, D.G., & Abadi, M.C. 19997, MNRAS, 286, 384

Toomre, A. 1977, in The Evolution of Galaxies and Stellar Populations, eds. B. Tinsley & R. Larson (New Have, CN: Yale Univ. Press)

Trager, S.C., Faber, S.M., Worthey, G., & González, J.J. 2000, AJ, 119, 1645

Wada, K., & Norman, C.A., 2001, ApJ, 574, 172

York D.G., et al., 2000, AJ, 120, 1579

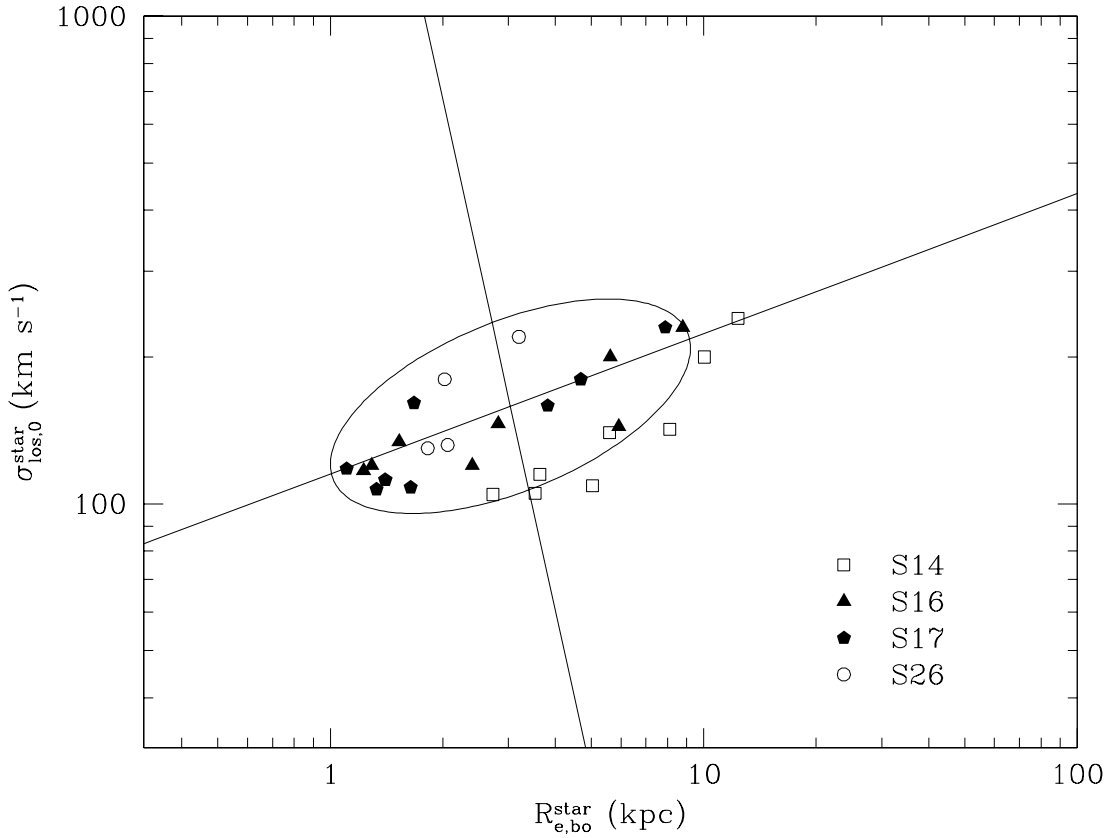

Fig. 1.— The central l.o.s. velocity dispersions of ELOs in the sample versus their stellar half-mass radii. Different symbols stand for different simulations. We also draw the concentration ellipse (with their major and minor axes) for the SDSS early-type galaxy sample from Bernardi et al. (2003b) in the z-band. See text for more details

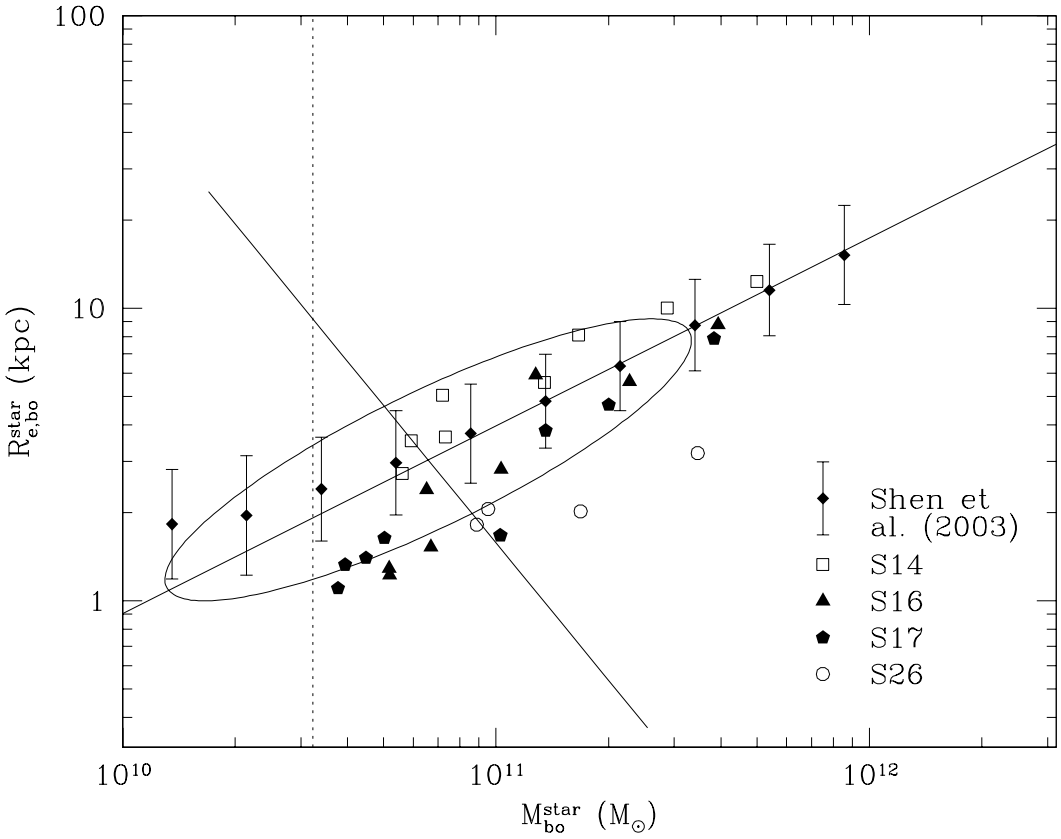

Fig. 2.— The projected stellar half-mass radii versus stellar masses. Filled diamonds with error bars correspond to median values of the Sérsic half-light radii in the z-band and their 1 sigma dispersions (Shen et al. 2003). We also draw the concentration ellipse for Bernardi et al.'s (2003b) sample in the z band and the lower limit for early-type-like galaxy stellar masses in the SDSS sample as found by Kauffmann et al. (2003b, dotted vertical line). See text for more details

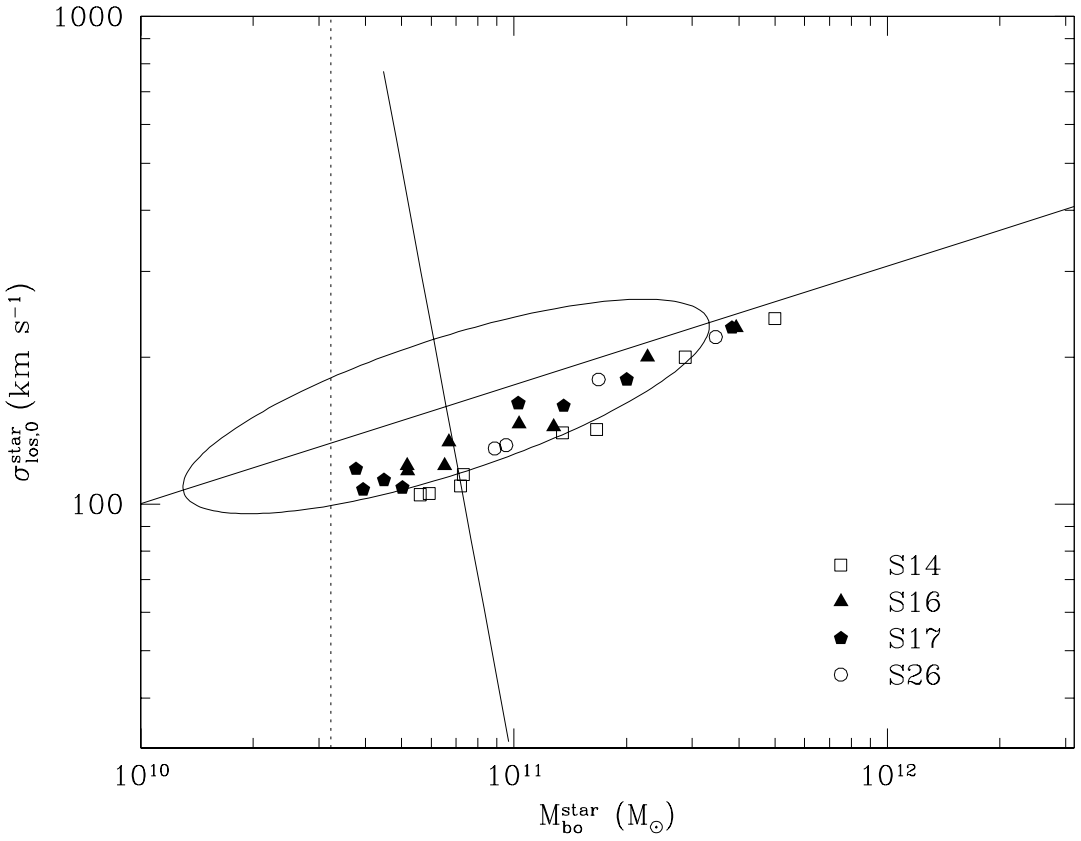

Fig. 3.— Same as Figure 1 for the central l.o.s. velocity dispersions versus stellar masses. Vertical line is as in Figure 2